Experimental (FT-IR, FT-Raman) and theoretical (HF and DFT) investigation and HOMO and LUMO analysis on the structure of p-fluoronitrobenzene

ARTICLE *in* SPECTROCHIMICA ACTA PART A MOLECULAR AND BIOMOLECULAR SPECTROSCOPY · SEPTEMBER 2011

Impact Factor: 2.35 · DOI: 10.1016/j.saa.2011.09.008 · Source: PubMed

4 AUTHORS, INCLUDING:

Sengeny Periandy
Independent Researcher
82 PUBLICATIONS **683** CITATIONS
SEE PROFILE

Mehmet Karabacak
Celal Bayar Üniversitesi
131 PUBLICATIONS **1,476** CITATIONS
SEE PROFILE

S. Ramalingam
A.V.C. College (Autonomous)
71 PUBLICATIONS **383** CITATIONS
SEE PROFILE

Spectrochimica Acta Part A 83 (2011) 575–586

Contents lists available at SciVerse ScienceDirect

Spectrochimica Acta Part A: Molecular and Biomolecular Spectroscopy

journal homepage: www.elsevier.com/locate/saa

Experimental (FT-IR, FT-Raman) and theoretical (HF and DFT) investigation and HOMO and LUMO analysis on the structure of p-fluoronitrobenzene

V. Udayakumar[a], S. Periandy[b], M. Karabacak[c], S. Ramalingam[d,*]

[a] Department of Physics, Thiru A. Govindaswamy Arts College, Tindivanam, Tamilnadu, India
[b] Department of Physics, Tagore Arts College, Puducherry, India
[c] Department of Physics, Afyon Kocatepe University, Afyonkarahisar, Turkey
[d] Department of Physics, A.V.C. College, Mayiladuthurai, Tamilnadu, India

ARTICLE INFO

Article history:
Received 20 July 2011
Received in revised form 19 August 2011
Accepted 1 September 2011

Keywords:
p-Fluronitrobenzene
FT-IR and FT-Raman
HOMO–LUMO
HF and DFT electronic spectra
Fundamental vibrational frequencies

ABSTRACT

FT-IR and FT-Raman spectra of p-fluoronitrobenzene ($FNO_2C_6H_4$) have been recorded in the region 4000–100 cm^{-1}. In this work, the experimental and theoretical spectra of p-fluoronitrobenzene (p-FNBz) are studied. The molecular geometry and vibrational frequencies are calculated in the ground state of molecule using ab initio Hartree–Fock (HF) and DFT (B3LYP and LSDA) methods with 6-31++G(d,p) and 6-311++G(d,p) basis sets. The computed values of frequencies are scaled to yield good coherence with observed values by using suitable factor. The complete assignments are performed on the basis of the total energy distribution (TED) of the vibrational modes, calculated with scaled quantum mechanics (SQM) method. The observed and calculated frequencies are found to be in very good agreement. The alteration of vibration bands due to the substitutions at the first and fourth position of the skeletal ring is also investigated from their characteristic region of linked spectrum. A study on the electronic properties, such as absorption wavelengths, excitation energy, dipole moment and frontier molecular orbital energies, are performed by time dependent DFT (TD-DFT) approach. The electronic structure and the assignment of the absorption bands in the electronic spectra of steady compounds are discussed. The calculated HOMO and LUMO energies show that charge transfer occurs within the molecule. The thermodynamic properties of the title compound at different temperatures have been calculated in gas phase, revealing the correlations between standard heat capacities (C) standard entropies (S), standard enthalpy changes (H) and temperatures.

1. Introduction

Benzene and its derivatives have been the subject of investigation for many reasons. Aromatic compound such as benzene derivative of p-Fluronitrobenzene is commonly used in pharmaceutical products. Fluorine substituent can greatly increase the fat solubility of molecules, which is particularly important in pharmaceuticals where it can increase their bioavailability. Including more fluorine amplifies the effect and have regular feature in both drug and agrochemical actives. Numerous common fungicides also contain fluorine atoms. Fluorine is a common element in antibiotic molecules, too. Fluorine has become a popular feature in drugs and agrochemicals because of the effects it exerts in molecules. The anti-inflammatory drugs are designed to treat rheumatoid arthritis [1].

Fluorine is the most electronegative atom of all the compounds. It pulls electrons towards it, thus reducing the electron density at the carbon in a C–F bond. It also affects the molecule's dipole moment and the molecule's overall stability. Nitrobenzene is an aromatic nitro compound. Most nitrobenzene (97%) is used in the manufacturing of aniline. Nitrobenzene is highly toxic in large quantities and is mainly produced as a precursor to aniline. In the laboratory it finds occasional use as a solvent especially for electrophilic [2].

Nitrobenzene can cause a wide variety of harmful health effects to exposed persons. Repeated exposures to a high concentration of nitrobenzene can result in a blood condition called methemoglobinemia (a form of anemia). This condition affects the ability of blood carrying oxygen [3]. Exposure level is extremely high nitrobenzene can cause coma and possibly death unless prompt medical treatment is received. In case of long-term exposure to nitrobenzene, the presence of its breakdown products, p-nitrophenol and p-aminophenol, in the urine is an indication of nitrobenzene exposure. The results of these tests cannot be used to determine the level of nitrobenzene exposure [4,5]. Therefore the

* Corresponding author. Tel.: +91 04364 222264; fax: +91 04364 222264.
E-mail address: ramalingam.physics@gmail.com (S. Ramalingam).

1386-1425/$ – see front matter.
doi:10.1016/j.saa.2011.09.008

fluorine substituted nitrobenzene is also used to produce pharmaceutical drugs and agrochemical products.

Various spectroscopic studies of halogen substituted compounds have been reported in the literature [6–16] from time to time. Vibrational spectra of fluorobenzene were studied extensively [17–19]. The molecular structure of orthofluoronitrobenzene has been investigated by gas-phase electron diffraction and ab initio MO calculations [20]. Literature survey reveals that to the best of our knowledge the detailed HF/B3LYP/LSDA comparative studies on the complete FT-IR and FT-Raman spectra of p-FNBz have not been reported so far. In this study, molecular geometry, optimized parameters, vibrational frequencies, HOMO (Highest occupied molecular orbital) and LUMO (Lowest unoccupied molecular orbital) energies, frontier orbital energy gap, dipole moment and thermodynamic properties at various temperatures are computed and the performance of the computational methods for HF, B3LYP, and LSDA at 6-31++G(d,p) and 6-311++G(d,p) basis sets are compared. These methods predict relatively accurate molecular structure and vibrational spectra with moderate computational effort. In particular, for polyatomic molecules the DFT methods lead to the prediction of more accurate molecular structure and vibrational frequencies than the conventional ab initio Hartree–Fock calculations. Among DFT calculation, Becke's three parameter hybrids functional combined with the Lee–Yang–Parr correlation functional (B3LYP) is the best predicting results for molecular geometry and vibrational wave numbers for moderately larger molecule [21–24].

The position of the substituents in the benzene ring plays a very important role on the structural and electronic properties of the molecule. p-FNBz molecule is di-substituted benzene; one F atom and NO_2 group. As a continuation of the interest in benzene derivative compounds, experimental and theoretical analyses are made in the present study. The results of this work are presented herein.

2. Experimental details

The compound under investigation namely p-FNBz is purchased from Sigma–Aldrich Chemicals, USA, which is of spectroscopic grade and hence used for recording the spectra as such without any further purification. The FT-IR spectrum of the compound is recorded in Bruker IFS 66 V spectrometer in the range of 4000–400 cm^{-1}. The spectral resolution is $\pm 2\ cm^{-1}$. The FT-Raman spectrum of same compound is also recorded in the same instrument with FRA 106 Raman module equipped with Nd:YAG laser source operating at 1.064 μm line widths with 200 mW power. The spectra are recorded in the range of 4000–100 cm^{-1} with scanning speed of 30 cm^{-1} min^{-1} of spectral width 2 cm^{-1}. The frequencies of all sharp bands are accurate to $\pm 1\ cm^{-1}$.

3. Computational methods

The first task for the computational work was to determine the optimized geometry of p-FNBz molecule. To determine conformational features of the molecule, the selected degree of torsional freedom, T (C3–C4–N12–O13), was varied from 0° to 360° in every 10° and the molecular energy profile is obtained with the B3LYP/6-311++G(d,p) method. And then the molecular structure of the title compound in the ground state is computed by performing both ab initio HF and DFT [B3LYP/LSDA] with 6-31++G(d,p) and 6-311++G(d,p) basis sets. The optimized structural parameters are used in the vibrational frequency calculations at HF and DFT levels. The minimum energy of geometrical structure is obtained by using level 6-31++G(d,p) and 6-311++G(d,p) basis sets. At the optimized geometry for the title molecule no imaginary frequency modes are obtained, so there is a true minimum on the potential energy surface is found. The calculated frequencies are scaled by 0.910, 0.905, 0.860, 0.820 and 0.960 for HF/6-31++G(d,p). For 6-311++G(d,p) basis set is scaled by 0.915, 0.862, 0.830 and 0.890. For B3LYP/6-31++G(d,p) set is scaled by 0.960, 0.935, 1.02 and 0.890. For 6-311++G(d,p) basis set is scaled by 0.962, 0.935, 0.910 and 1.030. For LSDA 6-31++G(d,p) basis set is scaled by 0.980, 0.930, 0.960, 1.03, 0.915 and 1.06. For LSDA 6311++G(d,p) basis set is scaled by 0.986, 0.960, 1.02, 0.930 and 1.08. All calculations for p-FNBz are performed using GAUSSIAN 03W program package on Pentium IV processor personal computer without any constraint on the geometry [25–28].

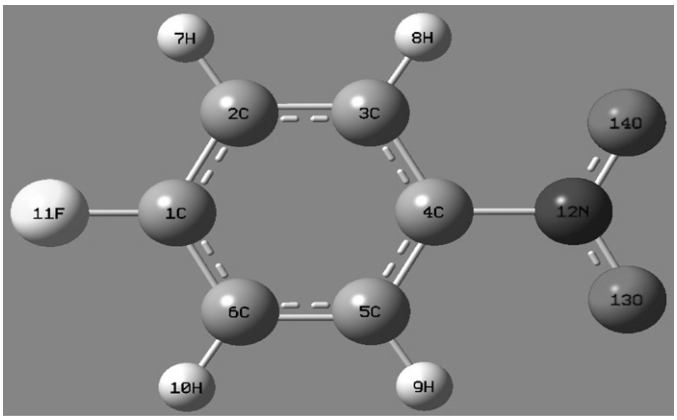

Fig. 1. Molecular structure and atom numbering scheme adopted in this study for p-FNBz.

Total energy distribution (TED) calculations, which show the relative contributions of the redundant internal coordinates to each normal vibrational mode of the molecule, and thus enable us numerically to describe the character of each mode were carried out by SQM method [29,30] using the output files created at the end of the frequency calculations. The TED calculations were performed by using PQS program [31].

The electronic properties, such as HOMO–LUMO energies, absorption wavelengths and oscillator strengths were calculated using B3LYP method of the time-dependent DFT (TD-DFT), basing on the optimized structure in solvent (DMSO and chloroform) and gas phase. Thermodynamic properties of the title compound at different temperatures have been calculated in gas phase using B3LYP/6-311++G(d,p) method.

4. Results and discussion

4.1. Molecular geometry and potential energy surface scan

The molecule contains nitro group and halogen atom F connected with benzene ring in the minimum of the potential energy surface, the substituent being co-planar with the ring the di-substituted derivative. The molecular structure of the p-FNBz belongs to C_{2v} point group symmetry. The optimized molecular structure of title molecule is obtained from GAUSSIAN 03 and GAUSSVIEW programs and is shown in Fig. 1 with numbering of the atoms. In particular, the effects of nitro groups are substituted in ortho, para and meta positions have been studied in many reactions. Generally these groups contribute two competing effects which control the reaction rate. First, a maximum activation through electron transfer is obtained if the nitro group is planar with the benzene ring. However spatial considerations often forbid this co-planarity in the case of ortho-substitution, and there exists a competing deactivation due to the twist of the nitro group from the plane of the benzene ring. In the extreme case of two ortho substituents, the activating effect of the nitro groups is greatly

diminished by this steric effect and may result in a net deactivation [32].

The structure optimization zero point vibrational energy of the title compound in HF, B3LYP, LSDA methods using 6-31++G(d,p) and 6-311++G(d,p) basis sets are 268728.8, 267044.0, 248666.1, 247310.8, 244423.6, 243101.5 J/mol and 64.22772, 63.82505, 59.43264, 59.10871, 58.41864, and 58.10265 kcal/mol, respectively. The comparative optimized structural parameters such as bond lengths, bond angles and dihedral angles are presented in Table 1. The ring appears little distorted and angles slightly out of perfect hexagonal structure. It is obviously due to the substitutions of the NO_2 group and halogen (F) group in the place of H atoms. The order of the optimized bond lengths of the six C–C bonds of the ring as C1–C2 = C1–C6 < C2–C3 = C5–C6 < C3–C4 = C4–C5. The N12–O13 and N12–O14 bond lengths are equal as compared to those bond lengths of nitro benzene [33].

The C–X (F, Cl, Br, etc.) bond length indicates a considerable increase when substituted in place of C–H. Therefore, the substitution with the F atom at the C which shares its π electron with the ring leads to some changes of the bond lengths and bond angles in the aromatic ring. This has been observed even in benzene derivatives [34,35]. Atom F is in the plane of the benzene ring. The C–F bond length value is calculated as 1.319–1.352 Å which is in good agreement with literatures [9,15,20]. The C–F bond length value for 1-bromo-3-fluorobenzene was observed as 1.342 Å [36]. The order of the optimized bond angles as C1–C2–C3 = C1–C6–C5 < C2–C3–C4 = C4–C5–C6 < C2–C1–C6 < C3–C4–C5.

In order to describe conformational flexibility of the title molecule, the energy profile as a function of C3–C4–N12–O13 (or C5–C4–N12–O14) torsion angle was achieved with B3LYP/6-311++G(d,p) method (Fig. 2). According to calculated T (C3–C4–N12–O13) is 0° for this method. The conformational energy profile shows two maxima near 90° and 270°. The maximum energies are obtained −536.132209909 and −536.132209974 Hartree for 90° and 270° dihedral angles, respectively. The aromatic rings are nearly perpendicular at these values of selected torsion angle. It is clear from Fig. 2, there are three local minima observed at 0°, 180° and 360° (−536.142373368 Hartree for 0°, −536.142373104 Hartree for 180°, −536.142373147 Hartree for 360°) for T (C2–C1–C16–C18). Therefore, the most stable conformer is for 0° torsion angle. The DFT optimized geometry of the crystal structure is coplanar at these values of selected torsion angle.

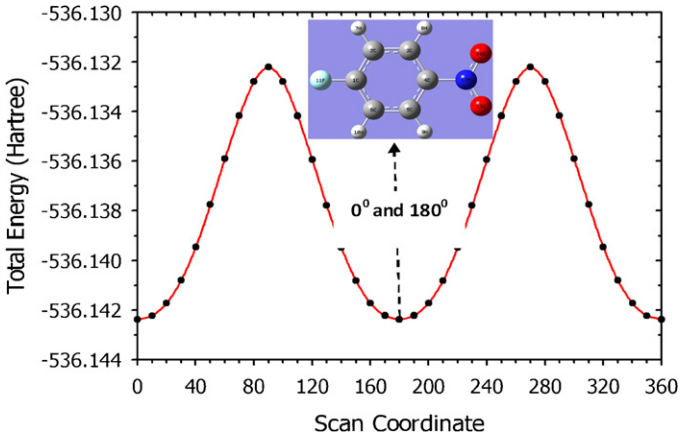

Fig. 2. PES scan for the selected torsional angle T(C3–C4–N12–O13) of freedom.

4.2. Vibrational assignments

The p-FNBz molecule consists of 14 atoms, which undergoes 36 normal modes of vibrations. On the assumption of a C_{2v} symmetry the numbers of vibration modes of the 36 fundamental vibrations of the molecule are distributed as

$$\Gamma_{Vib} = 13A_1 + 7B_1 + 4A_2 + 12B_2.$$

The assignments are shown in Table 2. The harmonic vibrational frequencies calculated for p-FNBz at HF and B3LYP/LSDA levels using the triple split valence basis set along with the diffuse and polarization functions, 6-31++G(d,p) and 6-311++G(d,p) observed FT-IR and FT-Raman frequencies for various modes of vibrations have been presented in Table 3. Comparison of frequencies calculated at HF and B3LYP/LSDA with the experimental values reveal the over estimation of the calculated vibrational modes due to

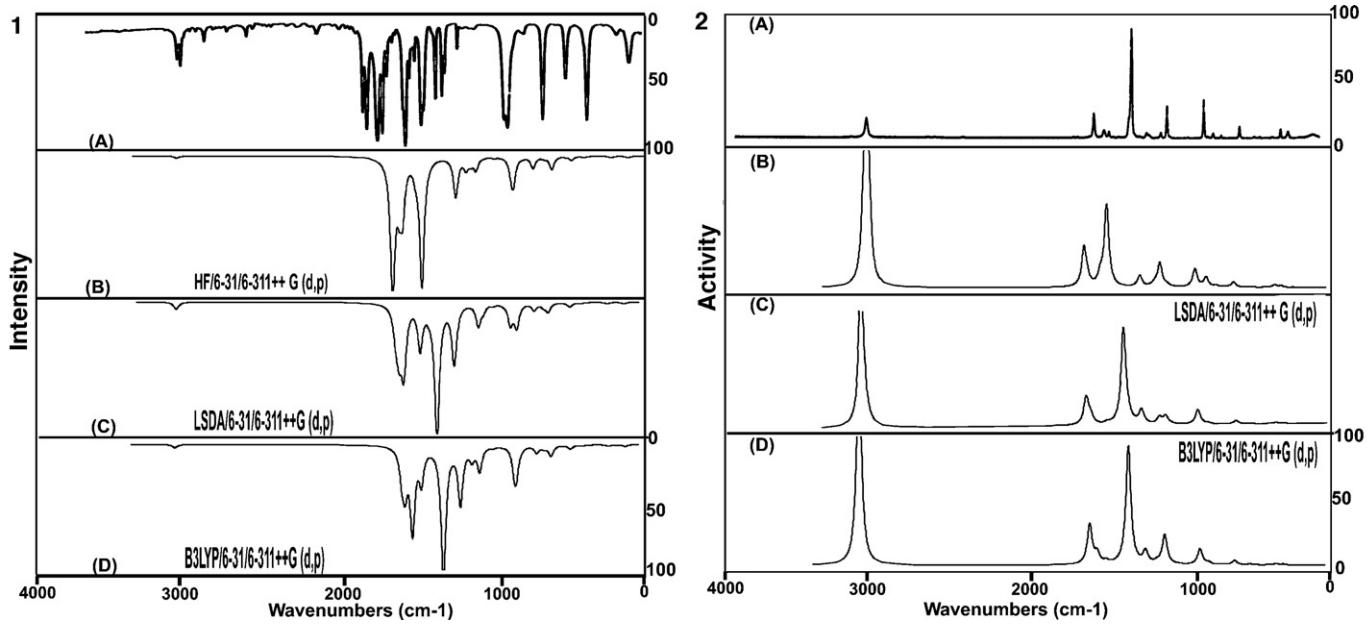

Fig. 3. (a) Experimental [A], calculated [B], [C] and [D] FT-IR spectra of p-fluoronitrobenzene. (b) Experimental [A], calculated [B], [C] and [D] FT-Raman Spectra of p-fluoronitrobenzene.

Table 1
Optimized geometrical parameters for p-Fluronitrobenzene computed at HF, B3LYP and LSDA methods, 6-31++G(d,p) and 6-311++G(d,p) basis sets.

Geometrical parameters	Methods					
	HF/6-31++G(d,p)	HF/6-311++G(d,p)	B3LYP/6-31++G(d,p)	B3LYP/6-311++G(d,p)	LSDA/6-31++G(d,p)	LSDA/6-311++G(d,p)
Bond length (Å)						
C1–C2	1.381	1.379	1.392	1.389	1.388	1.383
C1–C6	1.381	1.379	1.392	1.389	1.388	1.383
C1–F11	1.325	1.319	1.352	1.347	1.336	1.331
C2–C3	1.383	1.381	1.393	1.389	1.385	1.381
C2–H7	1.073	1.073	1.084	1.082	1.094	1.092
C3–C4	1.385	1.383	1.396	1.392	1.389	1.384
C3–H8	1.072	1.071	1.083	1.081	1.095	1.093
C4–C5	1.385	1.383	1.396	1.392	1.389	1.384
C4–N12	1.457	1.462	1.471	1.476	1.451	1.455
C5–C6	1.383	1.381	1.393	1.389	1.385	1.381
C5–H9	1.072	1.071	1.083	1.081	1.095	1.093
C6–H10	1.073	1.071	1.084	1.082	1.094	1.092
N12–O13	1.194	1.187	1.232	1.225	1.230	1.221
N12–O14	1.194	1.187	1.232	1.225	1.230	1.221
Bond angle (°)						
C2–C1–C6	122.88	122.72	122.91	122.76	122.97	122.79
C2–C1–F11	118.56	118.64	118.54	118.62	118.52	118.60
C6–C1–F11	118.56	118.64	118.54	118.62	118.52	118.60
C1–C2–C3	118.51	118.60	118.49	118.58	118.44	118.53
C1–C2–H7	119.93	119.87	119.92	119.85	119.61	119.55
C3–C2–H7	121.56	121.52	121.59	121.57	121.95	121.92
C2–C3–C4	119.02	119.05	118.98	119.00	118.81	118.86
C2–C3–H8	120.95	120.96	121.33	121.37	122.42	122.41
C4–C3–H8	120.02	120.00	119.69	119.63	118.77	118.74
C3–C4–C5	122.06	121.98	122.13	122.07	122.53	122.43
C3–C4–N12	118.97	119.01	118.93	118.96	118.73	118.78
C5–C4–N12	118.97	119.01	118.93	118.96	118.73	118.78
C4–C5–C6	119.02	119.05	118.98	119.00	118.81	118.86
C4–C5–H9	120.03	120.00	119.69	119.63	118.77	118.74
C6–C5–H9	120.95	120.96	121.33	121.37	122.42	122.41
C1–C6–C5	118.51	118.60	118.49	118.58	118.44	118.53
C1–C6–H10	119.93	119.87	119.92	119.85	119.61	119.55
C5–C6–H10	121.56	121.52	121.59	121.57	121.95	121.92
C4–N12–O13	117.63	117.58	117.74	117.64	117.56	117.39
C4–N12–O14	117.63	117.58	117.74	117.64	117.56	117.39
O13–N12–O14	124.74	124.84	124.53	124.72	124.89	125.21
Dihedral angles (°)						
C6–C1–C2–C3	0.0	0.0	0.0	0.0	0.0	0.0
C6–C1–C2–H7	180.0	180.0	180.0	180.0	180.0	180.0
F11–C1–C2–C3	180.0	180.0	180.0	180.0	180.0	180.0
F11–C1–C2–H7	0.0	0.0	0.0	0.0	0.0	0.0
C2–C1–C6–C5	0.0	0.0	0.0	0.0	0.0	0.0
C2–C1–C6–H10	180.0	180.0	180.0	180.0	180.0	180.0
F11–C1–C6–C5	180.0	180.0	180.0	180.0	180.0	180.0
F11–C1–C6–H10	0.0	0.0	0.0	0.0	0.0	0.0
C1–C2–C3–C4	0.0	0.0	0.0	0.0	0.0	0.0
C1–C2–C3–H8	180.0	180.0	180.0	180.0	180.0	180.0
H7–C2–C3–C4	180.0	180.0	180.0	180.0	180.0	180.0
H7–C2–C3–H8	0.0	0.0	0.0	0.0	0.0	0.0
C2–C3–C4–C5	0.0	0.0	0.0	0.0	0.0	0.0
C2–C3–C4–N12	180.0	180.0	180.0	180.0	180.0	180.0
H8–C3–C4–C5	180.0	180.0	180.0	180.0	180.0	180.0
H8–C3–C4–N12	0.0	0.0	0.0	0.0	0.0	0.0
C3–C4–C5–C6	0.0	0.0	0.0	0.0	0.0	0.0
C3–C4–C5–H9	180.0	180.0	180.0	180.0	180.0	180.0
N12–C4–C5–C6	180.0	180.0	180.0	180.0	180.0	180.0
N12–C4–C5–H9	0.0	0.0	0.0	0.0	0.0	0.0
C3–C4–N12–O13	180.0	180.0	180.0	180.0	180.0	180.0
C3–C4–N12–O14	0.0	0.0	0.0	0.0	0.0	0.0
C5–C4–N12–O13	0.0	0.0	0.0	0.0	0.0	0.0
C5–C4–N12–O14	180.0	180.0	180.0	180.0	180.0	180.0
C4–C5–C6–C1	0.0	0.0	0.0	0.0	0.0	0.0
C4–C5–C6–H10	180.0	180.0	180.0	180.0	180.0	180.0
H9–C5–C6–C1	180.0	180.0	180.0	180.0	180.0	180.0
H9–C5–C6–H10	0.0	0.0	0.0	0.0	0.0	0.0

the neglect of a harmonicity in real system. Inclusion of electron correlation in the density functional theory to certain extends makes the frequency values smaller in comparison with the HF frequency data. Reduction in the computed harmonic vibrations, although basis set sensitive is only marginal as observed in the DFT values using 6-311++G(d,p). Any way notwithstanding the level of calculations, it is customary to scale down the calculated harmonic frequencies in order to develop the agreement with the experiment. The scaled calculated frequencies minimize the root-mean square difference between calculated and experimental frequencies for

Table 2
Experimental FT-IR, FT-Raman frequencies (cm^{-1}) and assignments for p-FNBz.

Species C_{2v}	FT-IR frequency (cm^{-1}) and intensity	FT-Raman frequency (cm^{-1}) and intensity	Vibrational assignments
A_1	3120 s	–	(C–H) υ
B_2	3100 s	–	(C–H) υ
B_2	3090 s	3090 m	(C–H) υ
A_1	3070 w	–	(C–H) υ
B_2	1590 vs	1590 m	(C=C) υ
A_1	1530 vs	–	(C=C) υ
B_2	1500 vs	–	(NO_2) υ asym
A_1	1370 vs	–	(C=C) υ
B_2	1350 vs	1350 vs	(NO_2) υ sym
A_1	1320 s	–	(C–C) υ
B_2	1290 m	–	(C–F) υ
B_2	1160 vs	–	(C–C) υ
A_1	1150 vs	1150 w	(C–H) δ
A_1	1100 vs	1100 s	(C–H) δ
A_1	1090 vs	–	(C–H) δ
B_2	1060 w	–	(C–H) δ
A_1	1020 m	–	(C–N) υ
A_2	1015 w	–	(C–H) γ
B_1	1010 m	–	(C–H) γ
A_1	870 vs	870 s	(NO_2) δ
B_1	860 w	–	(C–H) γ
A_2	820 w	820 w	(C–H) γ
A_1	810 w	810 w	(CCC) δ
B_1	760 vs	–	(CCC) δ
B_1	720 vs	–	(NO_2) ω
B_2	610 vs	–	(C–N) δ
A_1	570 w	–	(CCC) δ
B_2	560 w	–	(NO_2) r
B_1	480 m	–	(CCC) γ
A_2	450 w	–	(CCC) γ
B_2	420 w	–	(CCC) γ
A_1	–	320 w	(C–F) δ
B_1	–	310 w	(C–N) γ
B_2	–	240 w	(C–F) γ
B_1	–	150 w	(NO_2) τ
A_2	–	100 w	(NO_2) τ

vs, very strong; s, strong; m, medium; w, weak; υ, stretching; δ, in plane bending; γ, out plane bending; τ, twisting:

bands with definite identifications. The descriptions concerning the assignment have also been indicated in Tables 2 and 3. For p-FNBz group the vibrational modes are C–H stretch, C–C stretch, C–F stretch, NO_2 group vibrations, C–N stretch and bending, C–H bends, C–F bending and C–C–C bending. The experimental and calculated FT-IR and FT-Raman spectra of the title molecule are presented in Fig. 3a and b respectively.

4.2.1. *Vibrational intensity analysis*

Computed vibrational spectral IR intensities and Raman activities of the title molecule for corresponding wave numbers by HF and DFT methods with B3LYP/LSDA with 6-31++G(d,p) and 6-311++G(d,p) basis sets have been collected in Table 4. In this case of IR intensities, the values are higher in HF than B3LYP whereas in the case of Raman activities the effect is reversed. The comparative graphs of IR intensities and Raman activities for five sets are presented in Figs. 4 and 5.

4.2.2. *C–H vibrations*

Aromatic compounds commonly exhibit multiple weak bands in the region 3100–3000 cm^{-1} due to aromatic C–H stretching vibrations which is the characteristic region for ready identification of this structure [33,37–40]. In this region, the bands are not affected appreciably by the nature of the substituents. Accordingly, in the present study, the four adjacent hydrogen atoms left around the ring the p-FNBz give rise four C–H stretching modes, four C–H in plane bending and four C–H out-of-plane bending vibrations which corresponds to stretching modes of C2–H7, C3–H8, C5–H9 and C6–H10 units. The vibrational modes 1–4 calculated to aromatic C–H stretch in the region 3080–3141 cm^{-1} are in agreement with experimental assignment at 3120s, 3100s, 3090s and 3070w cm^{-1} (FT-IR) and 3090 m cm^{-1} (FT-Raman) in the title molecule. The theoretically computed C–H vibrations by DFT/B3LYP and LSDA methods showed good agreement with recorded spectrum as well as the literature data. All aromatic C–H stretch modes are pure stretching modes as it is evident from TED column, they are almost 100%. This is indicating that the impact of substitution NO_2 group

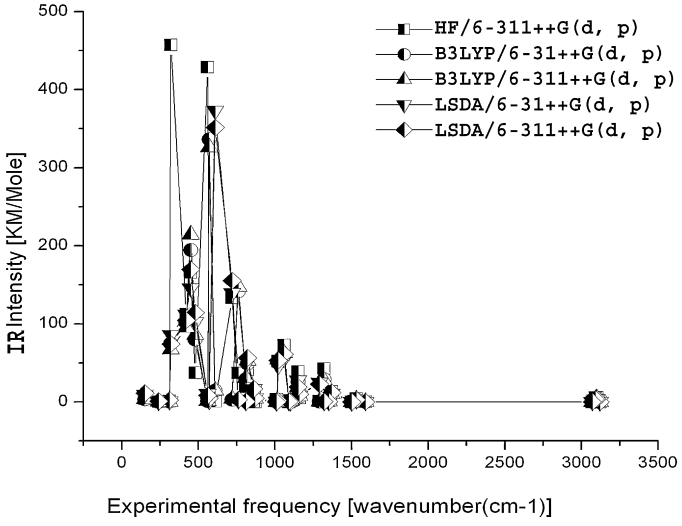

Fig. 4. Comparative graph of IR intensities by HF and DFT (B3LYP/LSDA).

Table 3
Calculated (HF/B3LYP/LSDA methods 6-31++G(d,p) and 6-311++G(d,p) level vibrational frequencies (cm^{-1}) of p-F4NBz.

S. No	Calculated frequency (cm^{-1})						Vibrational Assignments from B3LYP/6-311++G(d,p)
	HF/6-31++G(d,p) HF/6-311++G(d,p)		B3LYP/6-31++G(d,p)/B3LYP/6-311++G(d,p)		LSDA/6-31++G(d,p)/LSDA/6-311++G(d,p)		
	Unscaled value	Scaled value	Unscaled value	Scaled value	Unscaled value	Scaled value	TED (≥10%)
1	3421/3397	3113/3108	3246/3226	3116/3103	3162/3141	3099/3141	υ CH (100)
2	3421/3397	3113/3108	3246/3225	3116/3102	3161/3140	3098/3096	υ CH (100)
3	3392/3368	3087/3082	3226/3206	3097/3084	3152/3132	3089/3088	υ CH (100)
4	3391/3366	3086/3080	3225/3205	3096/3083	3151/3130	3088/3086	υ CH (100)
5	1842/1832	1584/1579	1663/1655	1596/1592	1662/1654	1596/1588	υ CC (70) + υ NO (12)
6	1793/1785	1542/1539	1642/1634	1535/1528	1639/1630	1524/1516	υ CC (68) + δ CCH (15)
7	1770/1761	1522/1518	1597/1583	1493/1480	1614/1600	1501/1488	υ NO_2 (80) asym
8	1673/1665	1372/1382	1528/1521	1360/1384	1497/1489	1370/1385	δ CCH (55) + υ CC (30)
9	1625/1619	1333/1344	1449/1443	1355/1349	1449/1432	1348/1332	υ CC (36) + δ CCH (30)
10	1564/1556	1345/1291	1382/1370	1327/1318	1430/1424	1330/1324	υ NO_2 (84) sym + υ CN (11)
11	1429/1422	1300/1301	1374/1358	1285/1306	1392/1376	1295/1280	υ CC (90)
12	1380/1376	1145/1142	1310/1307	1166/1189	1271/1260	1163/1242	δ CCH (85) + υ CC (10)
13	1318/1301	1133/1158	1259/1251	1177/1138	1236/1235	1149/1149	υ CF (50) + υ CC (20) + δ CCH (10)
14	1271/1266	1093/1091	1176/1173	1100/1097	1144/1138	1098/1092	δ CCH (60) + υ CC (13)
15	1234/1229	1117/1094	1126/1119	1081/1076	1101/1097	1101/1097	υ CC (28) + υ CN (25) + δ CCH (19)
16	1186/1176	1079/1047	1119/1116	1074/1074	1066/1063	1066/1063	δ CCH (68) + υ CC (26)
17	1114/1105	1014/1011	1028/1027	1028/1027	997/998	1027/1018	δ CCH (69) + υ CC (30)
18	1106/1101	1006/1007	988/987	1008/1017	947/946	1004/1022	γ CH (90)
19	1090/1074	992/983	975/966	995/995	939/929	995/1003	γ CH (82)
20	965/972	873/865	874/878	874/878	875/879	875/879	δ NO_2 (47) + ring breathing (42)
21	964/958	872/853	869/865	869/865	842/837	867/854	γ CH (85)
22	925/920	837/819	828/826	828/826	804/812	828/812	γ CH (99)
23	890/890	810/814	814/819	814/819	794/793	818/809	δ CCC (44) + δ NO (24) + υ CF (19)
24	845/815	769/746	748/726	763/748	740/720	762/778	Γ CCNO (81)
25	744/738	714/738	677/672	711/692	662/656	702/708	γ CCC (60) + Γ CCCH (35)
26	689/688	624/612	639/642	613/618	622/625	610/616	δ CCC (70) + δ CCF (10)
27	680/680	585/564	624/625	583/569	620/623	567/579	δ CCC (42) + υ CN (32) + υ CF (15)
28	578/580	555/580	534/536	561/552	530/533	562/576	r NO_2 (63) + δ CCN (14)
29	543/537	491/491	499/492	479/473	486/478	486/478	ω Ring (67) + Γ CCCF (13)
30	466/464	447/464	426/425	447/438	415/415	440/448	γ CCC (90)
31	445/447	427/409	408/409	416/421	399/402	423/410	δ CF (66) + δ CNO (12)
32	387/387	317/321	357/356	318/324	355/356	325/331	υ C–NO_2 (45) + δ CCC (13)
33	341/340	309/311	310/307	310/316	301/297	310/303	ω 1F4NBz (97) (γ CN + γ CF + γ CC)
34	251/250	241/240	228/228	239/235	225/225	239/243	r NO_2 (84) + δ CF (10)
35	130/129	125/129	116/114	122/117	113/111	120/120	ω NO_2 (56) + γ CF (17)+ Γ CCCC(14)
36	63/54	60/54	61/52	64/54	73/64	77/69	t NO_2 (98)

υ, stretching; δ, in plane bending; γ, out of plane bending; Γ, torsion; t, twisting; r, rocking; ω, wagging.

in the molecule which does not much influence the vibration of aromatic C–H. The strongest absorptions for aromatic compounds occur in the region 1000–650 cm^{-1} due to the C–H vibrations out of the plane to the aromatic ring [38–43]. In the present case, four C–H out-plane bending vibrations of the title compound are identify at 1015, 1010, 860 and 820 cm^{-1} (FT-IR) and 820 cm^{-1} (FT-Raman). The vibration modes 18, 19, 21 and 22 calculated to C–H out-plane bending vibrations are in agreement with experimental assignment. The TED for the out-of-plane bending vibrations are cal. 90%. In FT-Raman and FT-IR spectra the bands due to the C–H in-plane deformation vibrations occur in the region 1290–900 cm^{-1} [43]. In the present case, four C–H in-plane bending vibrations of the title compound are identified at 1150, 1100, 1090 and 1060 cm^{-1} (FT-IR), 1150 and 1100 cm^{-1} (FT-Raman). The TED for the in-plane bending vibrations are described as mixed modes. According to the literature, the in-plane and out-of-plane bending vibrational frequencies are found to be well within their characteristic region, which also support the previous observation in the case of C–H vibration. The above conclusions are in very good agreement with literature values [40–45]. The change in the frequencies of these deformations from the values in benzene is almost determined exclusively by the relative position of the substituents and is almost independent of their nature [46].

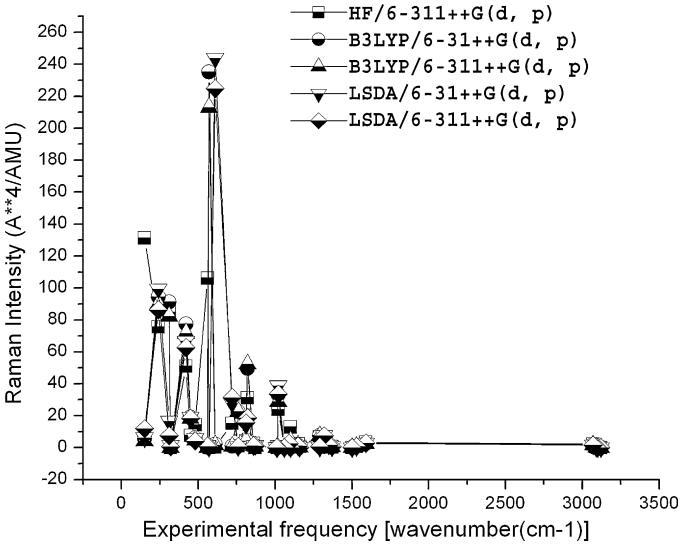

Fig. 5. Comparative graph of Raman intensity by HF and DFT (B3LYP/LSDA).

4.2.3. Fluorine vibrations

Assignments of the C–F stretching modes are very difficult as these vibrations are strongly coupled with the other in plane bending vibrations of several modes. Mooney [47] assigned the vibrations of the C–X group (X = F, Cl, Br, and I) in the wavenumber range of 1129–480 cm^{-1}. Normally [48–51], the observed bands of

Table 4
Comparative values of IR intensities and Raman Activities between HF/6-311++G(d,p), B3LYP/6-31++G(d,p), B3LYP/6-311++G(d,p), LSDA/6-31++G(d,p) and LSDA/6-311++G(d,p) basis sets of p-FNBz.

S. No	Calculated with HF/6-311++G(d,p)		Calculated with B3LYP/6-31++G(d,p)		Calculated with B3LYP/6-311++G(d,p)		Calculated with LSDA/6-31++G(d,p)		Calculated with LSDA/6-311++G(d,p)	
	IR Intensity (Ai)	Raman Activity (I)	IR Intensity (Ai)	Raman Activity (I)	IR Intensity (Ai)	Raman Activity (I)	IR Intensity (Ai)	Raman Activity (I)	IR Intensity (Ai)	Raman Activity (I)
1	0.0000	0.0079	0.0000	0.0173	0.0000	0.0085	0.0000	0.0452	0.0000	0.0320
2	5.6520	0.0160	4.8325	0.0062	4.7558	0.0018	4.0120	0.0190	3.8826	0.0089
3	5.5837	0.5124	3.8337	0.2127	3.9498	0.2438	3.4796	0.1454	3.5666	0.1685
4	0.0003	2.1723	0.0139	1.8313	0.0046	1.6944	0.0074	1.6414	0.0213	1.5106
5	0.0834	3.2786	0.1194	2.5898	0.2036	2.4813	0.0589	2.9919	0.1565	2.7593
6	4.4553	0.8662	3.2140	0.7881	3.1592	0.7685	2.6528	0.7353	2.5969	0.7167
7	0.0000	0.0142	0.0000	0.0038	0.0000	0.0066	0.0000	0.0051	0.0000	0.0070
8	13.1730	0.3684	8.6385	0.5865	10.2705	0.4933	10.3777	0.5560	12.0252	0.4945
9	1.7805	0.5773	0.6332	1.7123	0.6013	1.7552	0.4599	1.6548	0.4023	1.6834
10	42.5504	0.3950	28.9056	0.6079	27.3318	0.7080	0.3090	7.5600	0.3365	7.4027
11	1.0582	6.6629	0.4140	7.5453	0.4456	7.4080	25.0210	0.3409	22.6154	0.4651
12	5.1332	0.7335	6.6505	0.2453	7.8575	0.2047	7.8051	0.1623	9.5326	0.1495
13	38.7786	2.3546	25.7580	1.4091	18.6870	1.5155	27.5617	0.9331	18.8612	1.0004
14	2.1702	12.9022	0.0020	1.9182	1.0020	4.0663	0.0000	0.1201	0.0000	0.1002
15	0.0000	0.1726	0.0000	0.0001	0.0000	0.0000	0.0342	0.9236	0.5776	2.6304
16	72.9070	0.0002	58.8624	0.0005	62.7348	0.0170	55.6989	0.0049	61.2765	0.0521
17	52.2585	23.7906	49.9987	32.9441	54.4001	28.8079	46.2188	38.6910	53.1194	33.4419
18	0.6647	0.0423	0.6883	0.1372	1.0618	0.0855	1.1461	0.2807	1.8564	0.1689
19	3.1953	0.4820	0.0000	0.0011	0.0000	0.0010	0.0000	0.0051	0.0000	0.0055
20	0.0000	0.0004	4.5325	1.1957	4.4476	0.8085	4.8986	1.4370	4.7169	1.0760
21	0.8531	2.6940	10.1310	1.1798	10.3516	1.1458	16.4748	1.1458	16.7702	1.0686
22	40.6376	31.2579	49.0499	49.6037	52.8906	52.3688	51.4937	16.0373	56.4430	18.5923
23	19.4314	4.4486	28.6444	4.6971	30.7340	4.2421	0.3219	14.4464	0.3422	15.5201
24	36.9054	0.9830	142.0063	22.5450	147.7602	22.7396	2.5023	0.7348	2.8338	0.6883
25	133.1368	15.1490	2.8980	0.7192	3.8826	0.7337	139.7475	27.8658	155.4678	31.3532
26	0.5808	0.1589	14.3314	2.0350	14.5484	1.6913	373.4549	243.7939	351.3787	224.7328
27	2.4702	0.0154	336.4162	235.1509	326.2283	213.0346	1.4989	0.3067	4.4837	0.5822
28	428.7289	106.1122	0.8501	0.0562	1.3541	0.0694	10.2472	1.4088	8.1268	0.9094
29	37.2485	14.2448	79.8962	6.0899	85.9554	4.8036	102.4300	5.8349	114.3459	4.1032
30	165.9502	7.6089	194.3826	19.1317	214.5753	18.1664	145.8901	19.1911	169.6790	18.3643
31	112.4744	50.9360	100.9981	77.3236	95.2794	71.7141	112.3039	66.6615	104.6150	62.5844
32	457.1556	0.0005	74.7865	0.1039	67.3483	0.0034	86.0077	1.4406	74.3000	0.5974
33	0.8491	84.9307	0.5130	91.1123	0.2976	82.2993	1.2305	16.6182	2.4247	7.3678
34	0.2523	75.6217	0.0736	94.3422	0.0647	89.8618	0.4033	99.4489	0.9286	86.2545
35	4.1333	131.2909	3.1883	5.6781	3.5775	4.2666	9.4150	6.2676	11.0946	11.8140
36	3.0296	8.5838	4.6378	164.2118	5.0215	167.1993	5.5289	269.1270	5.0118	269.0005

the C–F stretching vibrations have been found to be very strong in the FT-IR spectra and these appear in the range 1000–1300 cm^{-1} for several fluoro-benzenes. Infrared spectra of substituted fluorine derivatives have assigned the wavenumber 1250 cm^{-1} to C–F stretching mode of vibration which has been studied by Narasimham et al. [52]. Karabacak et al. [9] have assigned the strong bands at 1254 and 1222 cm^{-1} in the FT-IR spectrum due to the C–F stretching mode. Sundaraganesan et al. [11] have assigned the strong bands at 1279 and 1331 cm^{-1} in FT-IR spectrum due to C–F stretching mode. Their counterpart in Raman spectrum is at 1280 and 1332 cm^{-1}. And also the C–F stretching vibration strongly coupled with the C–H in-plane bending vibrations, in the mono fluorinated benzene and is observed in the region 1100–1000 cm^{-1} [53]. The present molecule has one fluorine atom which is placed at para-position of the skeletal ring. Based on the above literature value, the corresponding C–F stretching vibration observed at 1290 cm^{-1} in FT-IR. According to the calculated TED (mode 13), our calculations show that there is no pure (C–F) band in this range. It is obviously seen from this results that the C–F stretching frequencies are slightly changed with the change of the position of F atoms.

The C–F in-plane bending vibration mode for the mono fluorinated benzene normally assigned at 250–350 cm^{-1} [54–56]. The band at 292 cm^{-1} in FT-Raman is assigned to C-F in-plane bending mode [11]. In the present case, a band assigned to C–F in-plane bending at 320 cm^{-1}. This view supported by the above literature. The frequency of the C–F out-of-plane bending vibration assigned at 240 cm^{-1}. According to the reported values [57], this assignment is in line with the literature. The C–F in-plane bending is observed to be enhanced by the substitution, though the same has suppressed the stretching.

4.2.4. C–C vibrations

The ring stretching vibrations are very much important in the spectrum of benzene and its derivatives are highly characteristic of the aromatic ring itself. The bands between 1400 and 1650 cm^{-1} in benzene derivatives are usually assigned to C=C stretching modes [42]. Varsanyi observed five bands, 1625–1590, 1590–1575, 1540–1470, 1465–1430 and 1380–1280 cm^{-1}, in this region [59]. In this title compound, the C=C stretching vibrations are found at 1590vs, 1530vs, 1370vs and 1320s cm^{-1} and the C–C stretching vibrations are assigned at 1592, 1528, 1349 and 1306 cm^{-1} (modes 5, 6, 9 and 11) by DFT/B3LYP/6-311++G(d,p). These assignments are in line with the literature. These vibrational positions are not very much affected by the nature of the substituents attached with the ring. The CCC in-plane bending vibrations are observed at 810, 760 and 570 cm^{-1} and the out-of-plane bending vibrations are appeared at 480, 450 and 420 cm^{-1}. The out-of-plane bending vibrations and other assignments are in good agreement with the literature [45,57,60]. According to TED results, mode 20 was assigned as ring breathing and NO_2 bending for title molecule.

4.2.5. Nitro group vibrations

The asymmetric stretching for the NO_2, NH_2 and CH_2 has a magnitude higher than that of the symmetric stretching [44].

Aromatic nitro compounds have strong absorptions due to the asymmetric and symmetric stretching vibrations of the NO_2 group at 1570–1500 cm^{-1} and 1370–1300 cm^{-1}, respectively [40,44]. Hydrogen bonding has a little effect on the NO_2 asymmetric stretching vibrations [57,58,61]. According to TED results, modes 7 and 10 were assigned as the NO_2 asymmetric and symmetric stretching for title molecule. In this title molecule, the strong bands at 1500vs and 1350vs cm^{-1} have been assigned to asymmetric and symmetric stretching modes of NO_2, respectively. The TED of these modes are contributing 80% for NO_2 asymmetric stretching and 84% for NO_2 symmetric stretching.

The other vibrations of NO_2 group (rocking, wagging and twisting) contribute to several normal modes in the low frequency region. Aromatic nitro compounds have a band of weak to medium intensity in the region 590–500 cm^{-1} [62] due to the out-of-plane bending deformation mode of the NO_2 group. This is observed at 560 cm^{-1} (calculated 561 cm^{-1}) for the title compound. The TED of this mode is 63% rNO_2 with 14% δCCN. Likewise, the in-plane NO_2 deformation vibrations have a week to medium absorption in the region 775–660 cm^{-1} [63,64]. In the present case, the NO_2 deformation (in plane bending and wagging) is observed at 870vs and 720vs cm^{-1}, respectively. The NO_2 torsional vibrations were observed in the infrared spectra at 250–159 cm^{-1}. Also the calculated twisting NO_2 vibrations (also called torsion around CN bond) were identified at 150w and 100w cm^{-1}. Hence it is clear that, this assignment is in line with the literature and the vibrational frequency is not affected. This is a unique occurrence of NO_2.

4.2.6. C–N vibrations

The identification of C–N vibrations is difficult task since the mixing of vibrations is possible in this region. The C–N stretching vibration is identify and assigned for title molecule 1020 cm^{-1} for infrared region. The TED for this mode suggests that this is a mixed mode. The assignments of C–N in-plane and out-of-plane bending vibrations are at 610 and 310 cm^{-1}, in this study the theoretical values are supported by the literature [40,65]. The remainder of the observed and calculated frequencies accounted in Tables 2 and 3.

4.3. UV–vis spectra analysis

Ultraviolet spectra analyses of p-FNBz have been investigated by theoretical calculation. In order to understand electronic transitions of compound, TD-DFT calculations on electronic absorption spectra in gas phase and solvent (DMSO and chloroform) are performed. The calculated frontier orbital energies, absorption wavelengths (λ), oscillator strengths (f) and excitation energies (E) for gas phase and solvent (DMSO and chloroform) are illustrated in Table 5. The major contributions of the transitions were designated with the aid of SWizard program [66]. Calculations of the molecular orbital geometry show that the visible absorption maxima of this molecule correspond to the electron transition between frontier orbitals such as translation from HOMO to LUMO. As can be seen from Table 5, the calculated absorption maxima values have been found to be 315.93, 296.32, 278.52 nm for gas phase, 316.10, 296.11, 278.68 nm for DMSO solution and 318.96, 289.61, 280.89 nm for chloroform solution at DFT/B3LYP/6-311++G(d,p) method. As can be seen, calculations performed at DMSO and chloroform are very close to each other when compared with gas phase. In view of calculated absorption spectra, the maximum absorption wavelength corresponds to the electronic transition from the highest occupied molecular orbital HOMO-2 to lowest unoccupied molecular orbital LUMO with 98% contribution. The other wavelength, excitation energies, oscillator strength and calculated counterparts with major contributions can be seen in Table 5.

4.4. HOMO–LUMO analysis

The total energy, energy gap and dipole moment have influence on the stability of a molecule. We have performed optimization in order to investigate the energetic behavior and dipole moment of title compound in solvent and gas phase. The total energy, dipole moment and frontier molecular orbital energies have been calculated with B3LYP/6-311++G(d,p) level. Results obtained in solvent and gas phase are listed in Table 6.

Highest occupied molecular orbital (HOMO) and lowest unoccupied molecular orbital (LUMO) are very important parameters for chemical reaction. We can determine the way the molecule interacts with other species; hence, they are called the frontier orbitals. The HOMO energy characterizes the ability of electron giving, LUMO characterizes the ability of electron accepting, and the gap between HOMO and LUMO characterizes the molecular chemical stability [67]. The energy gap between the highest occupied and the lowest unoccupied molecular orbitals, is a critical parameter in determining molecular electrical transport properties because it is a measure of electron conductivity. The energy values of HOMO are computed −7.82551, −7.88075 and −7.82279 eV and LUMO are −3.08634, −3.06539 and −3.08743 eV, and the energy gap values are 4.73917, 4.81536 and 4.73536 eV in DMSO, chloroform and gas phase for p-FNBz molecule, respectively. Surfaces for the frontier orbitals were drawn to understand the bonding scheme of present compound. In this work, the four important molecular orbitals (MO) for title molecule are examined: the second highest and highest occupied MOs and the lowest and the second lowest unoccupied MOs which we denote HOMO−1, HOMO, LUMO and LUMO+1, respectively. These MOs for gas phase are outlined in Fig. 6. The positive phase is red and the negative one is green. According to Fig. 6, the HOMO of 1F4NBz presents a charge density localized on the ring and on the NO_2 expect of N atom, but LUMO is characterized by a charge distribution on all molecule expect of some carbon atoms in the ring. The HOMO → LUMO transition implies an electron density transfer to NO_2 group from the ring. Moreover lower in the HOMO and LUMO energy gap explains the eventual charge transfer interactions taking place within the molecule. Furthermore, we can say that in going from the solvent phase to the gas phase, the dipole moment value increases (Table 6).

4.5. Thermodynamic properties

The values of some thermodynamic parameters (such as zero-point vibrational energy, thermal energy, specific heat capacity, rotational constants, entropy, and dipole moment) of p-FNBz molecule by HF, LSDA and B3LYP with 6-31++G(d,p) and 6-311++G(d,p) methods are listed in Table 7. The variation in zero-point vibrational energies (ZPVEs) seems to be significant. The ZPVE is much lower by the DFT/LSDA method than by the HF and B3LYP methods. The biggest value of ZPVE of 1F4NBz is 64.22772 kcal/mol obtained at HF/6-31++G(d,p). Whereas the smallest values is 58.10265 kcal/mol obtained at B3LYP/6-311++G(d,p).

On the basis of vibrational analysis at B3LYP/6-311++G(d,p) level, the standard statistical thermodynamic functions: standard heat capacities ($C^0_{p,m}$) standard entropies (S^0_m), and standard enthalpy changes (ΔH^0_m) for the title compounds were obtained from the theoretical harmonic frequencies and listed in Table 8.

From Table 8, it can be observed that these thermodynamic functions are increasing with temperature ranging from 100 to 700 K due to the fact that the molecular vibrational intensities increase with temperature [68]. The correlation equations between heat capacities, entropies, enthalpy changes and temperatures were fitted by quadratic formulas and the corresponding fitting factors (R^2)

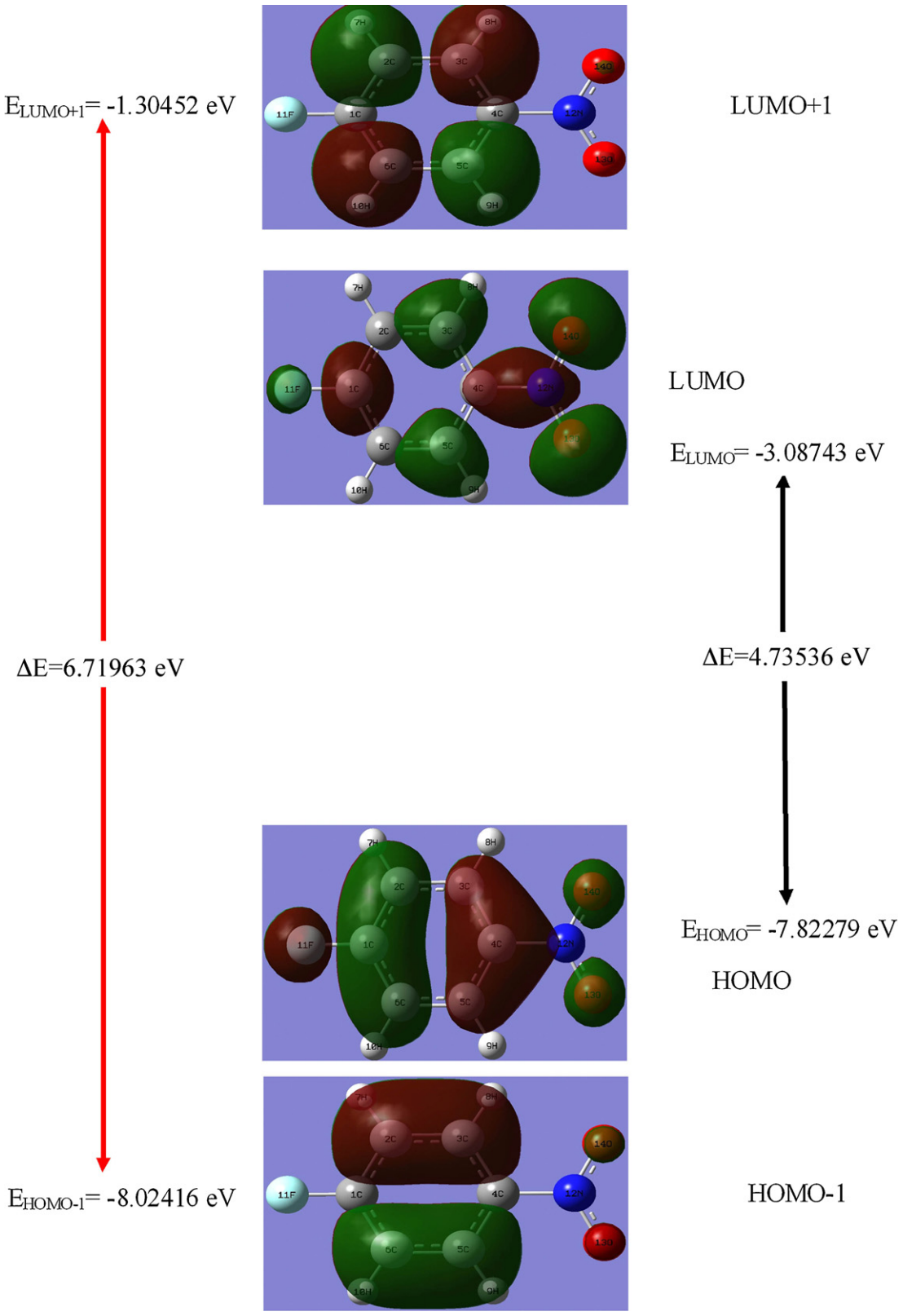

Fig. 6. The atomic orbital compositions of te frontier molecular orbital for p-FNBz.

Table 5
Theoretical electronic absorption spectra of p-FNBz (absorption wavelength λ (nm), excitation energies *E* (eV) and oscillator strengths (*f*)) using TD-DFT/B3LYP/6-311++G(d,p) method in gas and solvent (DMSO and chloroform) phase.

DMSO			Chloroform			Gas			Gas
λ (nm)	*E* (eV)	(*f*)	λ (nm)	*E* (eV)	(*f*)	λ (nm)	*E* (eV)	(*f*)	major contribution[a]
316.10	3.9223	0.0000	318.96	3.8872	0.0000	315.93	3.9244	0.0000	H-2 → L (98%)
296.11	4.1871	0.0147	289.61	4.2811	0.0148	296.32	4.1842	0.0139	H-1 → L (96%)
278.68	4.4490	0.0004	280.89	4.4140	0.0004	278.52	4.4515	0.0004	H-3 → L (98%)

[a] H, Homo, L, Lumo.

Table 6
Calculated energies values of p-FNBz in Gas and solvent (DMSO and chloroform) phase.

TD-DFT/B3LYP/6-311G(d,p)	DMSO	Chloroform	Gas
E_{total} (Hartree)	−536.006532854	−536.005538423	−536.00657039
E_{HOMO} (eV)	−7.82551	−7.88075	−7.82279
E_{LUMO} (eV)	−3.08634	−3.06539	−3.08743
$\Delta E_{HOMO-LUMO\ gap}$ (eV)	4.73917	4.81536	4.73536
E_{HOMO-1} (eV)	−8.02769	−8.10470	−8.02416
E_{LUMO+1} (eV)	−1.30833	−1.38698	−1.30452
$\Delta E_{HOMO-1-LUMO+1\ gap}$ (eV)	6.71936	6.71773	6.71963
Dipole moment μ (Debye)	4.18140	3.92880	4.19430

Table 7
The calculated thermo dynamical parameters of p-FNBz molecule in ground state at 298.15 K.

Basic set	HF 6-31++G(d,p)	HF 6-311++G(d,p)	LSDA 6-31++G(d,p)	LSDA 6-311++G(d,p)	B3LYP 6-31++G(d,p)	B3LYP 6-311++G(d,p)
SCF energy (a.u)	−533.04995128	−533.16457038	−533.24270102	−533.37048638	−536.01744983	−536.14237330
Zero point Vib. Energy (kcal/mol)	64.22772	63.82505	58.41864	58.10265	59.43264	59.10871
Rotational constants (GHz)	4.05430	4.07708	3.95139	3.98761	3.93662	3.96555
	0.81677	0.81790	0.81293	0.81588	0.79795	0.79991
	0.67982	0.68124	0.67422	0.67730	0.66347	0.66564
Specific heat (C_v) (cal mol^{-1} K^{-1})	26.463	26.604	29.295	29.387	28.762	34.941
Entropy (S) (cal mol^{-1} K^{-1})	84.532	84.907	86.523	86.852	86.477	86.876
Dipole moment μ (Debye)	3.4089	3.4116	3.4517	3.3567	3.3427	3.2812

Table 8
Thermodynamic properties at different temperatures at the B3LYP/6-311++G(d,p) level for p-FNBz molecule.

T (K)	$C^0_{p,m}$(cal mol^{-1} K^{-1})	S^0_m(cal mol^{-1} K^{-1})	ΔH^0_m(kcal mol^{-1})
100	11.673	64.538	1.058
150	15.587	70.793	1.836
200	19.975	76.443	2.823
250	24.532	81.833	4.034
298.15	28.871	86.876	5.416
300	29.035	87.068	5.473
350	33.314	92.175	7.133
400	37.264	97.151	8.998
450	40.837	101.984	11.052
500	44.029	106.664	13.275
550	46.863	111.186	15.647
600	49.376	115.546	18.154
650	51.605	119.747	20.779
700	53.590	123.793	23.509

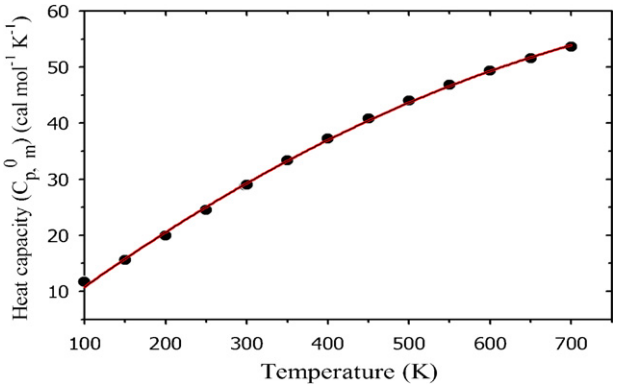

Fig. 7. Correlation graphic of heat capacity and tempreture of p-FNBz.

for these thermodynamic properties are 0.9991, 1.0000 and 0.9998, respectively. The corresponding fitting equations are as follows and the correlation graphics of those shown in Figs. 7–9.

$$C^0_{p,m} = 0.0073 + 0.1130\,T - 5.1375 \times 10^{-5}\,T^2 \quad (R^2 = 0.9991)$$

$$S^0_m = 52.7030 + 0.1243\,T - 3.2654 \times 10^{-5}\,T^2 \quad (R^2 = 1.0000)$$

$$\Delta H^0_m = -0.3035 + 0.0086\,T + 3.6738 \times 10^{-5}\,T^2 \quad (R^2 = 0.9998)$$

All the thermodynamic data supply helpful information for the further study on the p-FNBz. They can be used to compute the other thermodynamic energies according to relationships of thermodynamic functions and estimate directions of chemical reactions according to the second law of thermodynamics in Thermochemical field [69]. Notice: all thermodynamic calculations were done in gas phase and they could not be used in solution.

Dipole moment reflects the molecular charge distribution and is given as a vector in three dimensions. Therefore, it can be used as descriptor to depict the charge movement across the molecule. Direction of the dipole moment vector in a molecule depends on the centres of positive and negative charges. Dipole moments are strictly determined for neutral molecules. For charged systems, its value depends on the choice of origin and molecular orientation. As a result of HF and DFT (LSDA and B3LYP) calculations the highest dipole moment (3.4517 D) was observed for LSDA/6-31++G(d,p)

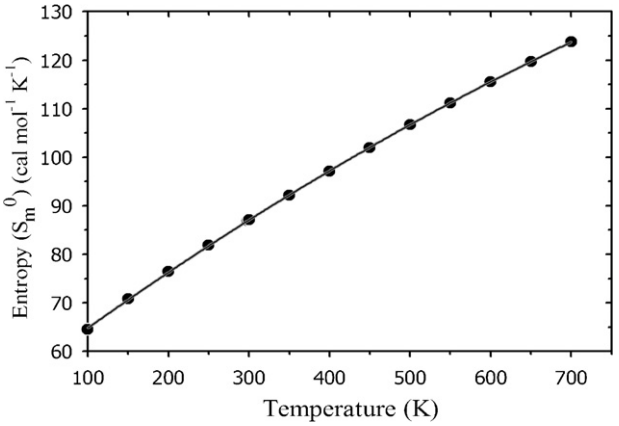

Fig. 8. Correlation graphic of entropy and tempreture of p-FNBz.

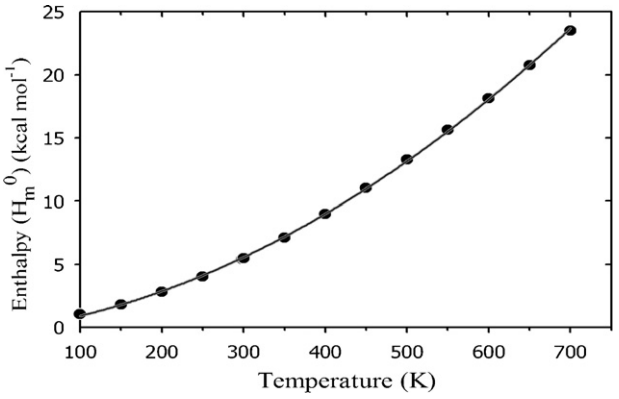

Fig. 9. Correlation graphic of enthalpy and tempreture of p-FNBz.

whereas the smallest one (3.2812 D) was observed for B3LYP/6-311++G(d,p) in p-FNBz.

5. Conclusion

The vibrational investigation on the structure and vibrational spectra, thermodynamic properties at various temperature, UV–vis spectral studies and Frontier molecular orbitals (FMOs), HOMO and LUMO analyses have been carried out on p-FNBz using HF and DFT (LSDA and B3LYP) calculations. Vibrational frequencies, infrared intensities and Raman activities are calculated by HF and DFT (LSDA and B3LYP) levels of theory utilizing 6-31++G(d,p) and 6-311++G(d,p) methods agree very well with experimental results. From the vibrational discussion, it is concluded that the substitution of H atom by F atom distort the ring geometries to small extent and the planarity of the molecule. The lowering of the HOMO–LUMO energy gap value has substantial influence on the intramolecular charge transfer and bioactivity of the molecule. The correlations between the statistical thermodynamics and temperature are also obtained. It is seen that the heat capacities, entropies and enthalpies increase with the increasing temperature owing to the intensities of the molecular vibrations increase with increasing temperature.

References

[1] http://www.reference.com/browse/nitrobenzene.
[2] http://msds.chem.ox.ac.uk/NI/nitrobenzene.html.
[3] www.jimmunol.org/content/156/5/1804.full.pdf.
[4] M.A. Palafox, F.J. Melendez, J. Mol. Struct. (Theochem) 625 (2003) 17–21.
[5] Q.G. Huang, L.R. Kong, Y.B. Liu, L.S. Wang, Relationships Between Molecular Structure and Chromosomal Aberrations In Vitro Human Lymphocytes Induced by Substituted Nitrobenzene, vol. 2, First edition, 1996.
[6] M. Karabacak, M. Çınar, A. Çoruh, M. Kurt, J. Mol. Struct. 919 (2009) 26–33.
[7] S. Ramalingam, S. Periandy, B. Elanchezhian, S. Mohan, Spectrochim. Acta A 78 (2011) 429–436.
[8] V. Mukherjee, N.P. Singh, R.A. Yadav, Spectrochim. Acta A 77 (2010) 787–794.
[9] M. Karabacak, E. Kose, M. Kurt, J. Raman Spectrosc. 41 (2010) 1085–1097.
[10] W. Lewandowski, M. Kalinowska, H. Lewandowska, Inorg. Chim. Acta 358 (2005) 2155–2166.
[11] N. Sundaraganesan, B. Anand, C. Meganathan, B.D. Joshua, Spectrochim. Acta A 68 (2007) 561–566.
[12] G. Thakur, V.B. Sing, N.L. Sing, Indian J. Pure Appl. Phys. 7 (1969) 107.
[13] S. Mohan, P. Feridoun, Indian J. Pure Appl. Phys. 24 (1986) 570.
[14] R.B. Sing, D.K. Rai, Indian J. Pure Appl. Phys. 20 (1982) 330.
[15] V. Krishnakumar, V. Balachandran, Spectrochim. Acta A 61 (2005) 1001–1006.
[16] H.M. Badawi, W. Förner, Spectrochim. Acta A 71 (2008) 388–397.
[17] V.J. Eaton, D. Steele, J. Mol. Spectrosc. 48 (1973) 446.
[18] R.A.R. Pearce, D. Steele, K. Radcliffe, J. Mol. Spectrosc. 15 (1973) 409.
[19] E.D. Lipp, C.J. Seliskar, J. Mol. Spectrosc. 73 (1978) 290.
[20] I.F. Shishkov, L.V. Khristenko, L.V. Vilkov, S. Samdal, S. Gundersen, Struct. Chem. 14 (2) (2003) 151–157.
[21] A.D. Becke, Phys. Rev. A 38 (1988) 3098.
[22] C. Lee, W. Yang, R.G. Parr, Phys. Rev. B 37 (1988) 785.
[23] A.D. Becke, J. Chem. Phys. 98 (1993) 5648.
[24] S. Ramalingam, S. Periandy, M. Govindarajan, S. Mohan, Spectrochim. Acta A 75 (2010) 1308–1314.
[25] D.C. Young, Computational Chemistry: A Practical Guide for Applying Techniques to Real World Problems (Electronic), John Wiley & Sons Inc., New York, 2001.
[26] N. Sundaraganesan, S. Ilakiamani, H. Saleem, P.M. Wojiciechowski, D. Michalska, Spectrochim. Acta A 61 (2005) 2995.
[27] Gaussian 03 Program, Gaussian Inc., Wallingford, CT, 2004.
[28] M.J. Frisch, A.B. Nielsen, A.J. Holder, Gauss View Users Manual, Gaussian Inc., Pittsburg, PA, 2000.
[29] J. Baker, A.A. Jarzecki, P. Pulay, J. Phys. Chem. A 102 (1998) 1412–1424.
[30] SQM version 1.0, Scaled Quantum Mechanical Force Field, 2013 Green Acres Road, 18 Fayetteville, Arkansas 72703.
[31] E. Runge, E.K.U. Gross, Phys. Rev. Lett. 52 (1984) 997–1000.
[32] V. Krishnakumar, N. Prabhavathi, Spectrochim. Acta A 72 (2009) 738–742.
[33] V. Krishnakumar, V. Balachandran, T. Chithambarathan, Spectrochim. Acta A 62 (2005) 918–925.
[34] M. Karabacak, A. Çoruh, M. Kurt, J. Mol. Struct. 892 (2008) 125–131.
[35] J.R. Durig, T.S. Little, T.K. Gounev, J.K. Gargner Jr., J.F. Sullivan, J. Mol. Struct. 375 (1996) 83.
[36] A.A. Knapik, W. Minor, M. Chruszcz, Acta Crystallogr. E64 (2008) o466.
[37] N. Puviarasan, V. Arjunan, S. Mohan, Turkey J. Chem. 26 (2002) 323.
[38] G. Varsanyi, Vibrational Spectra of Benzene Derivatives, Academic Press, New York, 1969.
[39] V. Krishnakumar, R.J. Xavier, Indian J. Pure Appl. Phys. 41 (2003) 597.
[40] M. Silverstein, G. Clayton Bassler, C. Morrill, Spectrometric Identification of Organic Compounds, Wiley, New York, 1981.
[41] A.J. Abkowicz-Bienko, D.C. Bienko, Z. Latajka, J. Mol. Struct. 552 (2000) 165–175.
[42] T.F. Ardyukoiva, et al., Atlas of Spectra of Aromatic and Heterocyclic Compounds, Nauka Sib. otd., Novosibirsk, 1973.
[43] J. Mohan, Organic Spectroscopy—Principles and Applications, second ed., Narosa Publishing House, NewDelhi, 2001.
[44] D. Lin-Vien, N.B. Colthup, W.G. Fateley, J.G. Grasselli, The Handbook of Infrared and Raman Characteristic Frequencies of Organic Molecules, Academic Press, Boston, MA, 1991.
[45] A. Altun, K. Gölcük, M. Kumru, J. Mol. Struct. (Theochem) 637 (2003) 155.
[46] N. Sundaraganesan, H. Saleem, S. Mohan, Spectrochim. Acta A 59 (2003) 2511.
[47] E.F. Mooney, Spectrochim. Acta 20 (1964) 1021.
[48] V.J. Eatch, D. Steel, J. Mol. Spectrosc. 48 (1973) 446–449.
[49] R.A.R. Pearce, D. Steel, K.J. Radcliffe, J. Mol. Struct. 15 (1973) 409–414.
[50] M.P. Kumpawat, A. Ojha, N.D. Patel, Can. J. Spectrosc. 25 (1980) 1.
[51] L.J. Bellamy, The Infrared Spectra of Complex Molecules, vol. 2, Chapman and Hall, London, 1980.
[52] N.A. Narasimham, M.Z. El-Saban, J. Rud-Nielson, J. Chem. Phys. 24 (1956) 420.
[53] I.L. Tocon, M. Becucci, G. Pietraperzia, E. Castellucci, J.C. Otero, J. Mol. Struct. 565 (2001) 421–425.
[54] M. Honda, A. Fujji, E. Fujimaki, T. Ebata, N. Mikami, J. Phys. 7 (1969) 250–254.
[55] K. Shashidar, R.K. Suryanarayana, E.S. Jayadevappa, Spectrochim. Acta 26 (1970) 2373.
[56] M.S. Navti, M.A. Shashidar, Indian J. Phys. 668 (1994) 371–373.
[57] N. Sundaraganesan, C. Meganathan, B. Domnic Joshua, P. Mani, A. Jayaprakash, Spectrochim. Acta A 71 (2008) 1134–1139.
[58] D.N. Sathyanarayana, Vibrational Spectroscopy Theory and Application, NewAge International Publishers, New Delhi, 2004.
[59] G. Varsanyi, Assignments of Vibrational Spectra of 700 Benzene Derivatives, Wiley, New York, 1974.
[60] M. Ramalingam, N. Sundaraganesan, H. Saleem, J. Swamanathan, Spectrochim. Acta A 71 (2008) 23–30.
[61] N. Sundaraganesan, S. Ilakiamani, H. Saleem, P.M. Wojieehowski, D. Michalska, Spectrochim. Acta A 61 (2005) 2995.

[62] S. George, Infrared, Raman Characteristics Group Frequencies, Tables and Charts, 3rd edition, Wiley, Chichester, 2001.
[63] V. Krishnakumar, V. Balachandran, Spectrochim. Acta A 61 (2005) 1811–1819.
[64] R.A. Kanna Rao, N. Syam Sundar, Spectrochim. Acta 49A (1993) 1691.
[65] S. Mohan, N. Sundaraganesan, J. Mink, Spectrochim. Acta A 47 (1991) 1111.
[66] S.I. Gorelsky, SWizard Program Revision 4.5., University of Ottawa, Ottawa, Canada, 2010, http://www.sg.chem.net/.
[67] K. Fukui, Science 218 (1982) 747.
[68] J. Bevan Ott, J. Boerio-Goates, Calculations from Statistical Thermodynamics, Academic Press, 2000.
[69] R. Zhang, B. Dub, G. Sun, Y. Sun, Spectrochim. Acta A 75 (2010) 1115–1124.